

## Supporting Information

# Intracellular Nanoparticle Dynamics Affected by Cytoskeletal Integrity

*Martha E. Grady<sup>‡†§</sup>, Emmabeth Parrish<sup>‡§</sup>, Matthew A. Caporizzo<sup>§</sup>, Sarah C. Seeger<sup>‡§</sup>, Russell J.*

*Composto<sup>§||</sup>, David M. Eckmann<sup>\*‡||</sup>*

### AUTHOR ADDRESS

<sup>‡</sup> Department of Anesthesiology and Critical Care, School of Medicine,  
University of Pennsylvania  
3620 Hamilton Walk, Philadelphia, PA 19104, USA

<sup>§</sup> Department of Materials Science and Engineering, School of Engineering and Applied Science,  
University of Pennsylvania  
3231 Walnut Street, Philadelphia, PA 19104, USA

### Contents

#### Experimental methods and materials

<i>Cell culture</i> .....	1
<i>Tubulin and actin visualization</i> .....	1
<i>Cell injection</i> .....	2
<i>Particle tracking</i> .....	3
<i>Quantum dot characterization</i> .....	4

#### Particle tracking results

<i>MSDs and tracks of QDs within each cell type and condition</i> .....	5
<i>Alpha distributions of QDs within each cell type and condition</i> .....	8
<i>Van Hove distributions of QDs within each cell type and condition</i> .....	10

<b>Supplemental movie</b> .....	13
---------------------------------	----

<b>References</b> .....	14
-------------------------	----

## Experimental methods and materials

### Cell culture

Two cell lines were cultivated for this study: human dermal fibroblasts and HT 1080 (fibrosarcoma cells). Fibroblasts were cultured in Fibrolife (Lifeline Cell Technologies). HT 1080 fibrosarcoma cells were cultured in DMEM L-glutamine supplemented with 10% fetal bovine serum and 1% penicillin streptomycin. All cells were incubated at 37 °C in a humidified atmosphere with 5% CO<sub>2</sub>. Cells were grown to confluency and harvested by trypsinization. Dishes and coverslips were coated for 30–40 min with 5 µg/mL fibronectin (BD Biosciences) dissolved in PBS prior to plating. Cells were initially plated at 75-100k density on glass coverslips (22 x 40 mm) for all studies, and were incubated for 48 hrs prior to experiments. Three conditions were studied: control (recording buffer only), 2.5 µM Cytochalasin D (Sigma Aldrich) in recording buffer for 30 min, and 10 µM Nocodazole (Sigma Aldrich) in recording buffer for 30 min. Recording buffer solution was made as follows: 10% 10x HBSS (Gibco), 1% Heparin, 1% Glutamax, and 1% FBS in DI water. Solution was then pH-balanced to 7.4 using NaOH.

### Tubulin and actin visualization

Cells were incubated in 250 nM TubulinTracker Green (Life Technologies) for 30 min at 37°C, then rinsed three times, and placed in recording buffer for fluorescence imaging with a standard FITC filter. For actin visualization, cells were fixed with 4% paraformaldehyde (Electron Microscopy Sciences, Hatfield, PA; diluted with HBSS from a 16% stock solution) for 15 min, then permeabilized for 3 min with 0.1% Triton, followed by 20 min of dye-loading with 100 nM Acti-stain 488 phalloidin (Cytoskeleton, Inc, Denver, CO) taken from a 14 µM stock prepared according to the manufacturer's instructions. Images were taken on an Olympus IX 51 with a 40x oil-immersion objective. See Grady *et al.*<sup>1</sup> for additional images.

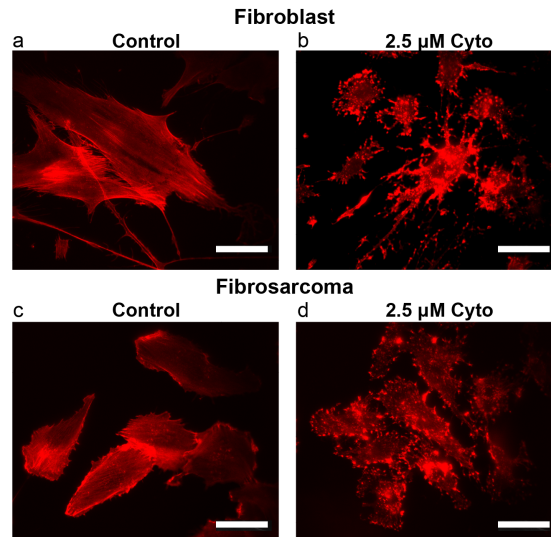


**Figure S1.** Effect of cytoskeletal destabilizer, cytochalasin D (Cyto), on fibroblasts (a,b) and fibrosarcoma cells (c,d). Images taken at 40 x magnification. Scale bars are 50 µm.

### Cell injection

QDs entered the cells through our microinjection system shown in Figure S2. A Nikon Eclipse Ti inverted fluorescence microscope is paired with an Eppendorf InjectMan4 micromanipulator and Eppendorf FemtoJet4i pressure injector. QDs were dispersed in DI water at 0.2 nM concentration and loaded into Eppendorf Femtotips with outer diameter of 1  $\mu\text{m}$  and inner diameter of 0.7  $\mu\text{m}$ . Smaller inner diameters increased the occurrence of tip blockage resulting in discarding more tips. Input pressure varied with use of the tip. Ideally, after injection, the tip would remain unblocked and the same input pressure could be used throughout all experiments. However, higher input pressures needed to be used to adjust for partial blockage of the tip after subsequent cell injection from debris. Typical input pressure values used were 200-400 hPa. To balance for capillary action of the buffer solution being drawn into the injection tip, a back pressure is applied to the needle. Typical value for back pressure was 5 hPa. Because the viscosity of the injection fluid closely matches that of the buffer solution, an exact back pressure to balance capillary action was elusive. Instead, the back pressure was modulated between 5 hPa, the lowest non-zero setting, and 0 hPa so that the needle did not leak QDs into the surrounding buffer solution. An x-y stage mounted to the microscope platform allowed the movement of the cell-coated coverslip into different viewing windows.



**Figure S2.** Experimental set up with inverted optical microscope, nanoinjector, micromanipulator, and monitor displaying injection needle and fibroblast cells at 40x.

Experiments ranged over multiple days with control dishes of each cell line experimented on the same day as drug-treated dishes. Multiple cells were injected from a single dish. Number of cells for each condition and the number of particle tracks are included in Table S1.

**Table S1.** Number of cells and particle tracks for each cell line and drug condition. Fibroblasts (Fibro) and fibrosarcoma cells (FSarcoma) under control conditions, cytochalasin D treatment (Cyto) and nocodazole treatment (Noco).

Cell Type	Drug Condition	# Cells	# Particle Tracks
Fibro	Control	28	699
	Cyto	14	353
	Noco	25	600
FSarcoma	Control	27	634
	Cyto	18	408
	Noco	14	314

### *Particle tracking*

Videos were recorded in brightfield before injection, then fluorescence just after injection, and finally brightfield again to examine the cell. Particle tracking software, FIESTA, was used to extract particle tracks from the fluorescence signature of QDs within the recorded videos. For consistency, 1000 frames were analyzed corresponding to ~1 min at a frame rate of 16.9 fps. The calibration of the objective is 110 nm per pixel. Though the size of the QD cores are 4 nm, the fluorescence signatures of the QDs are much larger than one pixel. The FIESTA program applies a Gaussian fit to the fluorescence to determine the center of the fluorescence with nm precision. Maximum pixel size for a particle was set at 70 pixels, however the full width half max of the fluorescence was initialized at 900 nm (approximately 8 pixels). Max velocity was set at 15  $\mu\text{m/s}$  to preclude tracking particles within the buffer solution. Additionally, a selection box was used to identify approximate cell boundaries and to limit the run time of the program by excluding areas outside of the cell from analysis. Drift was evaluated using immobilized QDs and found to be on the order of error in positioning. Particle tracks with an average positioning error greater than 25 nm were excluded from analysis. The minimum number of frames was set at 10 and the max break was set at 4 frames. A jump tolerance between individual frames of 1000 nm was added to preclude connectivity between adjacent particles. These values were found by analyzing a single video at a range of values for maximum break (2, 4, 6, 8), max velocity (10, 15, 20  $\mu\text{m/s}$ ), and jump tolerance (500, 1000 nm).

### *Quantum dot characterization*

Core size of the CdSe core/ZnS shell QDS3 was measured using ImageJ software on TEM images such as Figure S3. The oleic acid ligand of QDs was exchanged with thiol terminated 5 kDa MW PEG. The exchange was confirmed by FTIR, the particles dispersion in water, and the increased separation between QDs observed in TEM images. QD diffusion in a solution of 90 wt% glycerol in water was measured to determine the hydrodynamic radius of the PEGylated QDs from the Stokes-Einstein relationship between diffusion coefficient and particle size. Other studies have shown that this method results in hydrodynamic radii similar to DLS values.<sup>2</sup> The addition of the PEG ligand to the surface of the particles added ~3 nm to each side of the QD, resulting in a

hydrodynamic diameter of 10 nm. The increased separation observed via TEM for neighboring QDs is comparable to the measured increase in the hydrodynamic diameter.

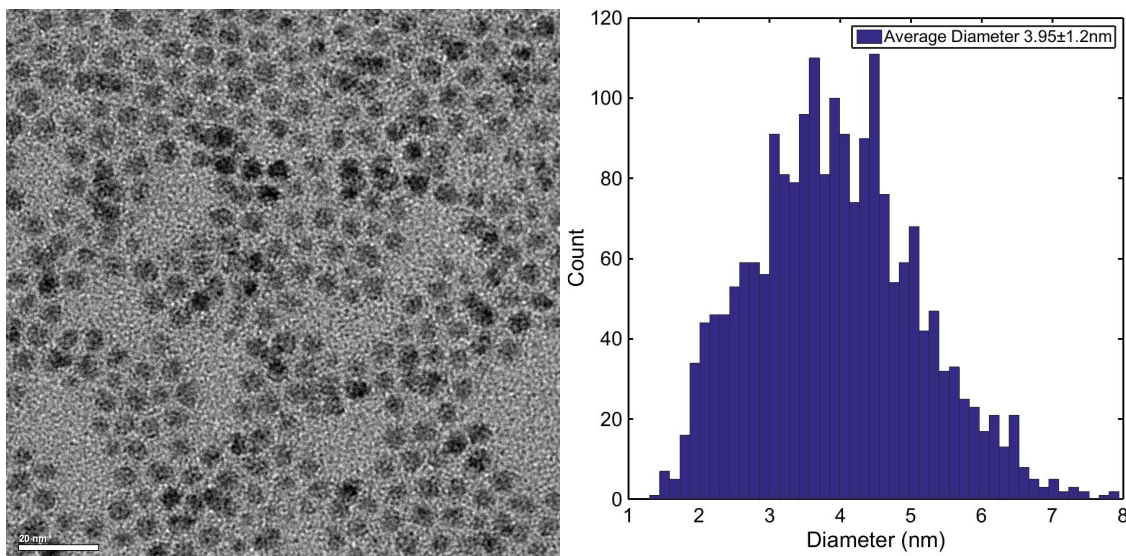


**Figure S3.** TEM image of quantum dots used in the study (left) and histogram of measured diameters (right).

## Particle tracking results

### *MSDs and tracks of QDs within each cell type and condition*

Particle tracks listed in Table S2 appear initialized at (0,0) for within fibroblasts in Figure S4a-c and for within fibrosarcoma cells in Figure S5a-c for each drug condition: cytochalasin D (Cyto) and nocodazole (Noco). Corresponding MSDs for all particle tracks are included in the bottom row (Figure S4d-f and Figure S5d-f) with the appropriate color scale extending throughout both figures. The color scale allows the eye to distinguish differences in the spread of the MSDs over a long time scale, which is further quantified by examining the MSD spread at a particular time as in Figure S6 ( $t = 1$  s). Figure S4 and S5 show time delays over two decades from 0.1 s to 10 s. In reality, there are MSDs that persist for longer delay times. However, a common artifact to SPT is that MSDs will tend to flatten at longer times. This effect is due to particle loss from the imaging plane and is evidenced by trajectories with higher MSDs that persist for shorter times. Faster moving QDs will diffuse out of the imaging plane quicker and will result in a downturn in the average MSD at longer times. Therefore, we have limited the delay time displayed in the geometric mean of all six conditions (main text Figure 5) to only 2 s so as not to be biased toward slower moving particles.

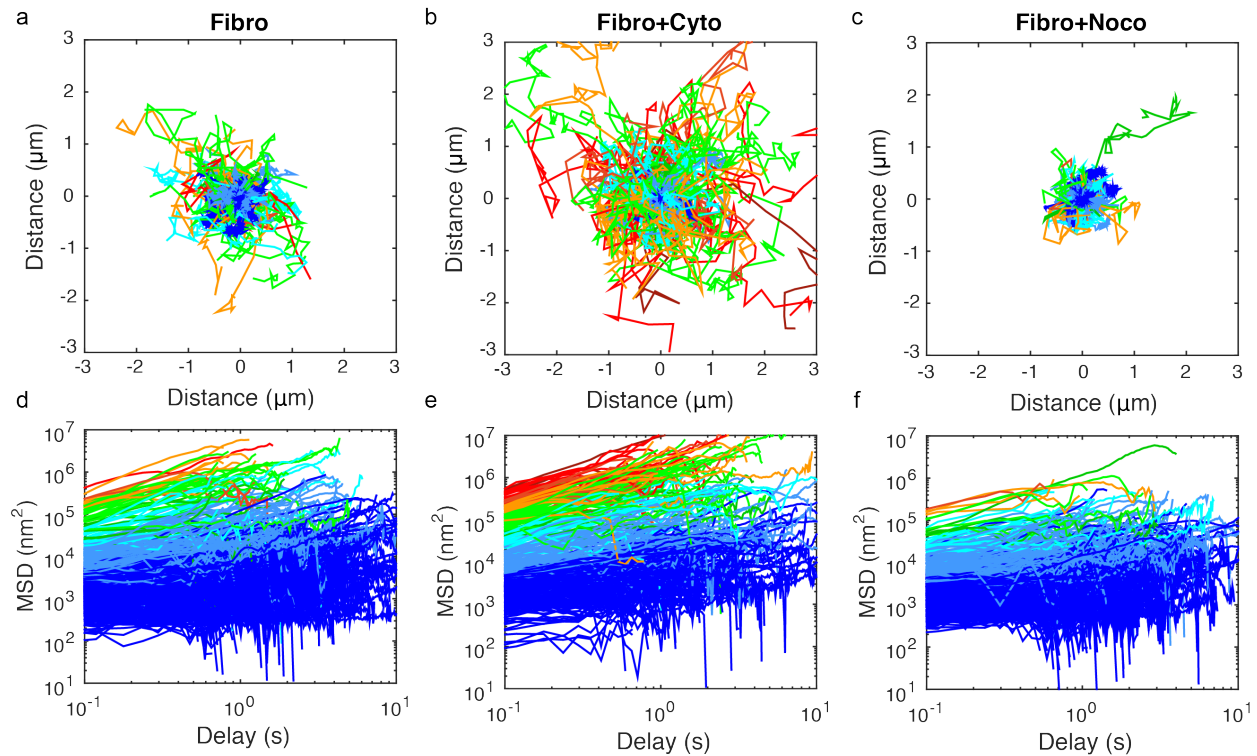


**Figure S4.** Track overlays (a-c) and MSDs (d-f) calculated for QDs within fibroblasts (a,d), fibroblasts treated with cytochalasin D (b,e) and fibroblasts treated with nocodazole (c,f). Color scale used to indicate higher MSD is consistent throughout Figures S4 and S5.

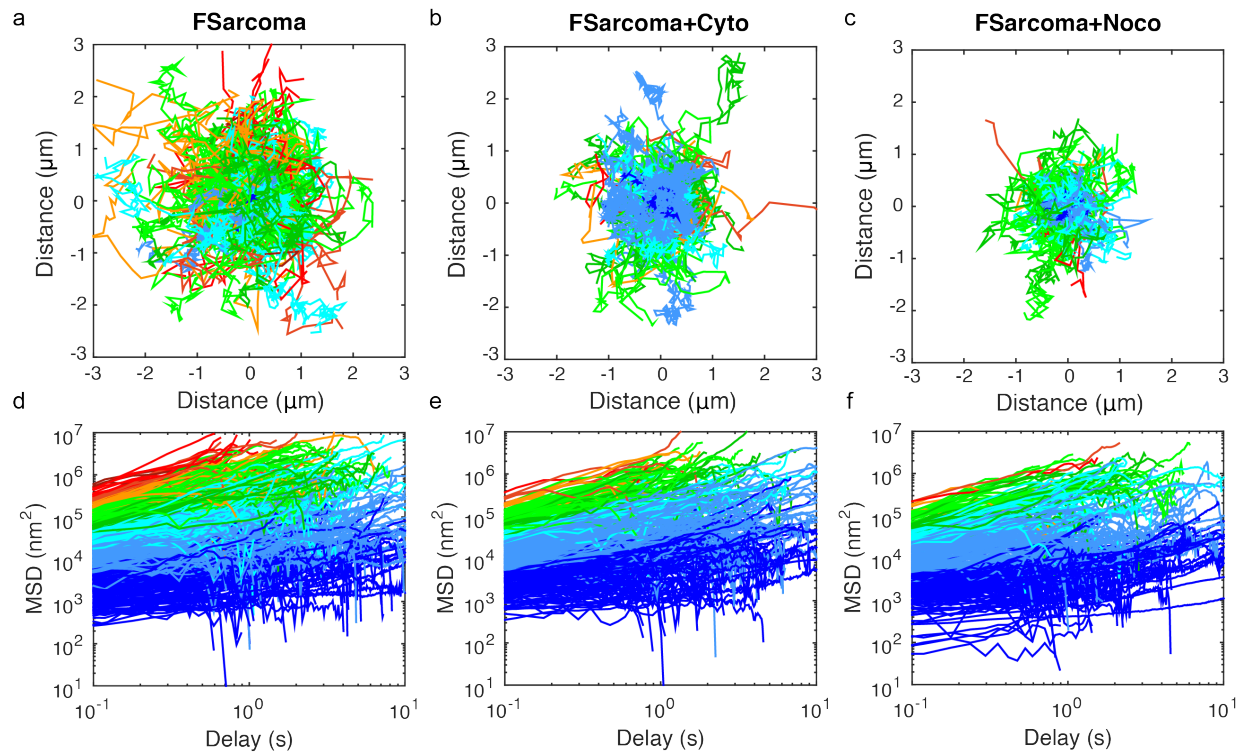


**Figure S5.** Track overlays (a-c) and MSDs (d-f) calculated for QDs within fibrosarcoma cells (a,d), fibrosarcoma cells treated with cytochalasin D (b,e) and fibrosarcoma cells treated with nocodazole (c,f). Color scale used to indicate higher MSD is consistent throughout Figures S4 and S5.

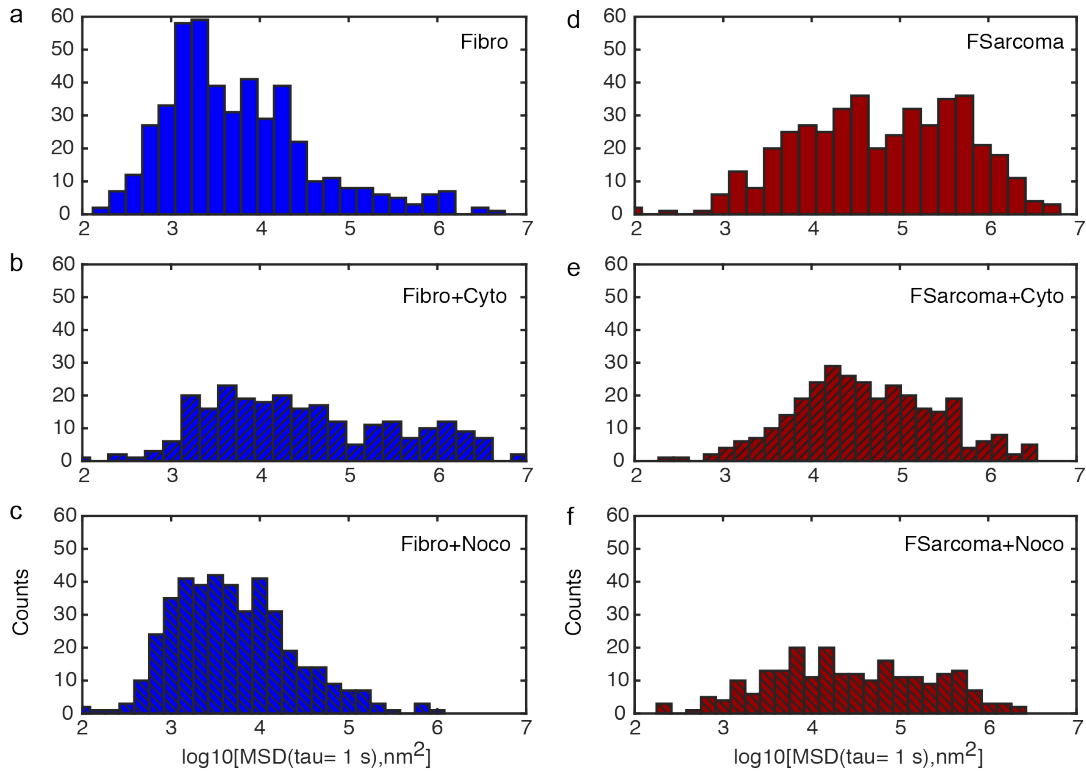


**Figure S6.** Histogram of log of MSDs at a delay time of 1 s for QDs within (a) fibroblasts, (b) fibroblasts with cytochalasin D treatment, (c) fibroblasts with nocodazole treatment, (d) fibrosarcoma cells, (e) fibrosarcoma cells with cytochalasin D treatment, and (f) fibrosarcoma cells with nocodazole treatment.

*Alpha distributions of QDs within each cell type and condition*

In order to extract diffusion coefficients, we examined a subset of the captured data. The number of tracks that pass each sorting condition are given in Table S3. The number of tracks that fit the power law,  $MSD = 2Dt^\alpha$ , with an  $r^2 > 0.7$ , correspond to a subset of total tracks. Further sorting was based on the power law exponent, alpha, being close to freely diffusive motion, between 0.75 and 1.25. These limits were chosen based on the standard deviation of alphas from QDs within the glycerol solution. The resulting diffusion coefficients (column 5, Table S2) were extracted from a linear fit to each track that meets both a power law fit to the MSD and alpha close to 1 (column 4, Table S2).

Overall, QDs tended toward subdiffusive behavior rather than Brownian motion. However, more QDs within the fibrosarcoma cell cytoplasm experienced Brownian motion as the center of the alpha distribution is much closer to 1 (Figure S7d) valued at 0.75, than the center of the alpha distribution of QDs within fibroblasts at 0.60 (Figure S7 a). The application of cytochalasin D shifted the center of the alpha distribution slightly higher to 0.70 for QDs within fibroblasts and had little effect on QDs within fibrosarcoma cells, shifting the alpha distribution center only slightly lower to 0.72. Nocodazole treatment generally shifted alpha distributions lower from control values to 0.56 within treated fibroblasts and to 0.66 for treated fibrosarcoma cells.

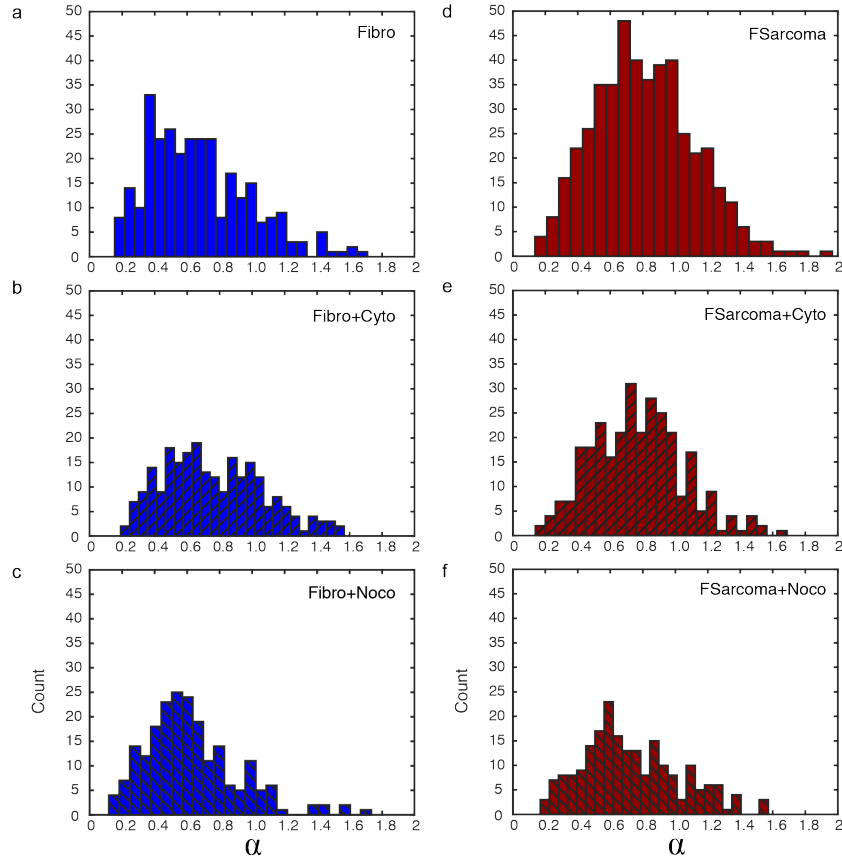


**Figure S7.** Histogram of alpha exponent from power law fit for QDs within (a) fibroblasts, (b) fibroblasts with cytochalasin D treatment, (c) fibroblasts with nocodazole treatment, (d) fibrosarcoma cells, (e) fibrosarcoma cells with cytochalasin D treatment, and (f) fibrosarcoma cells with nocodazole treatment.

**Table S2.** Sorting results from power law fit of MSDs to extract diffusion coefficients for each cell line and drug condition. Fibroblasts (Fibro) and fibrosarcoma cells (FSarcoma) under control conditions, cytochalasin D treatment (Cyto) and nocodazole treatment (Noco).

Cell Type	Total # of tracks	Power law tracks $r^2 > 0.7$	Diffusive tracks $0.75 < \alpha < 1.25$	Diffusion coefficient ( $\text{nm}^2/\text{s}$ )
Fibro	699	300	85	3.86E+04
Fibro+Cyto	353	236	96	1.34E+05
Fibro+Noco	600	212	49	1.65E+04
FSarcoma	634	458	208	8.63E+04
FSarcoma+Cyto	408	294	142	5.11E+04
FSarcoma+Noco	314	210	76	6.45E+04

### *Van Hove distributions of QDs within each cell type and condition*

Displacement distributions for each cell line are shown in Figure S8. The increased mobility of QDs observed via the particle trajectories and MSD of fibroblast cells exposed to cytochalasin D and fibrosarcoma cell line is echoed in the increased occurrences of larger displacements. The dual nature of these distributions, central peaks with exponential tails gives indication to the dichotomy of the QD behavior caused by confinement imposed by the actin and microtubule networks. Quantification of the tail characteristic length is obtained by exponential fitting of both the positive and negative tails, given in Table S3 along with the non-Gaussian parameters,  $N_g$ . Example fitting of the positive tail and center Gaussian peak at 0.12 s can be seen in Figure S9 for QDs within fibroblasts with cytochalasin D treatment. The characteristic lengths provide information about the localization imposed by the cytoskeletal networks. Namely, greater confinement of the QDs is associated with smaller characteristic lengths, as these relate to rare jumps out of localization. The  $N_g$  values of the cell lines show that more open cytoskeletal networks correspond to a shift toward Gaussian behavior and more dynamic homogeneity.

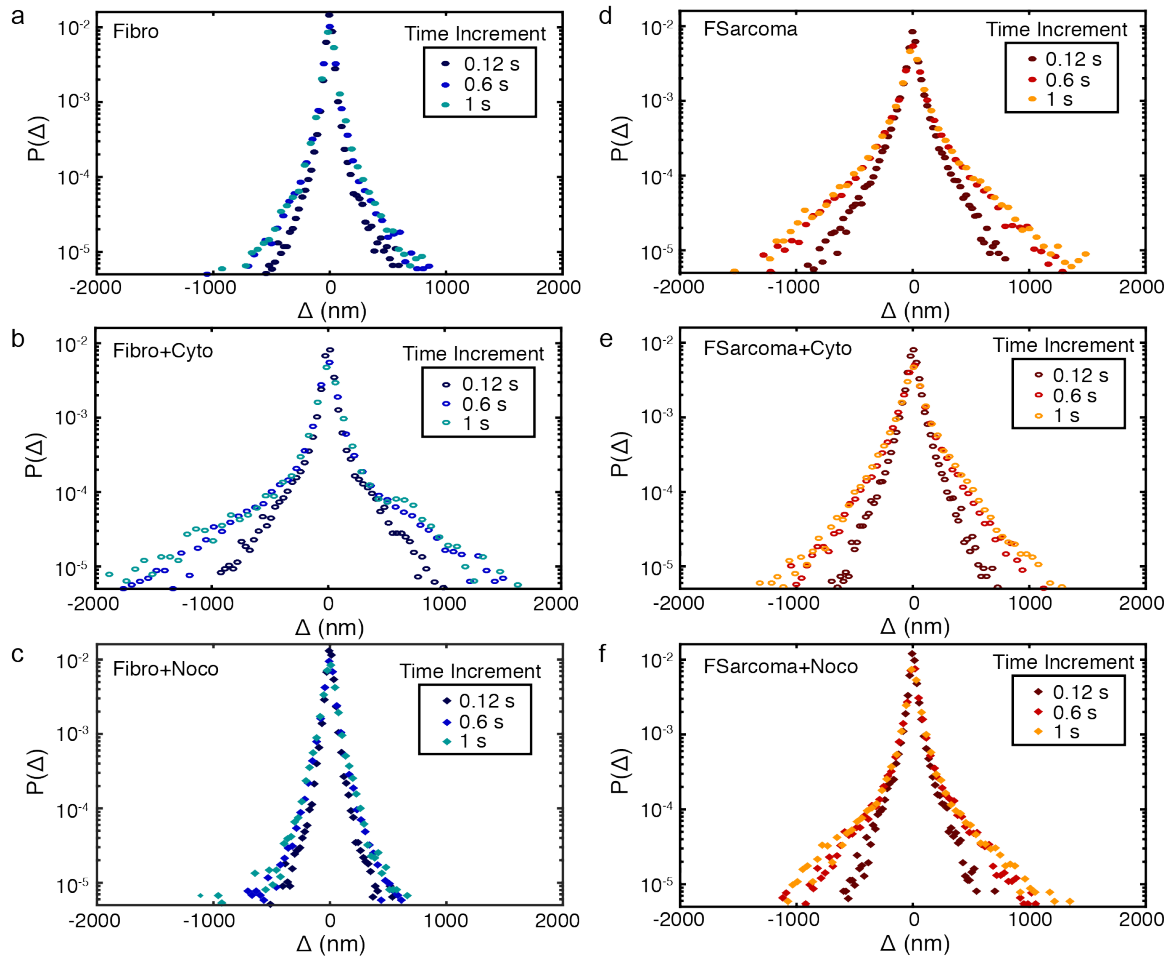


**Figure S8.** van Hove distributions of QD steps within (a) fibroblasts, (b) fibroblasts with cytochalasin D treatment, (c) fibroblasts with nocodazole treatment, (d) fibrosarcoma cells, (e) fibrosarcoma cells with cytochalasin D treatment, and (f) fibrosarcoma cells with nocodazole treatment. Displacements between three time increments of 0.12 s, 0.6 s, and 1 s are included. Panels a, b and d appear as Figure 4 a, c, b in the main text, respectively.

**Table S3.** Non-Gaussian parameters and characteristic lengths from van Hove distributions.

Cell Type	Time (s)	Non-Gaussian Parameter, $N_g$	Characteristic Length (nm)
Fibro	0.12	14.7	96.0
	0.6	19.7	101.2
	1.0	21.5	114.9
Fibro+Cyto	0.12	6	192.9
	0.6	7.3	297.6
	1.0	7.4	328.4
Fibro+Noco	0.12	10.2	89.6
	0.59	15.5	101.4
	1.01	13.5	104.6
FSarcoma	0.12	3.8	129.4
	0.6	5.1	187.0
	1.0	5	224.4
FSarcoma+Cyto	0.12	3.6	108.2
	0.6	4.2	157.2
	1.0	4.1	166.7
FSarcoma+Noco	0.12	4.8	98.1
	0.6	5.4	140.5
	1.0	5.7	141.5

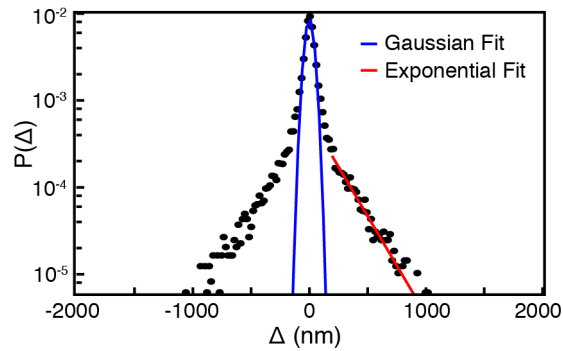


**Figure S9.** Characteristic lengths are extracted from an exponential fit (red line) to the tail portion of the van hove distribution plotted for QDs within fibroblasts with cytochalasin D treatment. Both positive and negative tails are included in the exponential fit.

### Supplemental images and movie

A representative image of a fibrosarcoma cell after injection is shown in Figure S10. The QDs are indicated by arrows, the nucleus is indicated by dashed line and the cell boundary is indicated by a red dashed line. One representative movie of a fibrosarcoma control cell was chosen, cropped for length of time and compressed for availability online. Injection can be seen in brightfield followed by fluorescence of the quantum dots. Still images with particle tracks overlaid from before injection and 2 minutes post-injection are included in Figure S11.

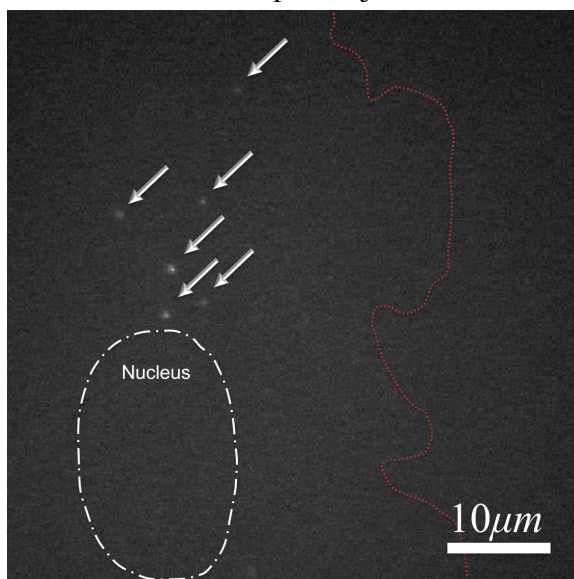


**Figure S10.** Still OM image with QDs indicated by arrows. Nucleus and cell periphery are indicated by dashed white and red lines, respectively.

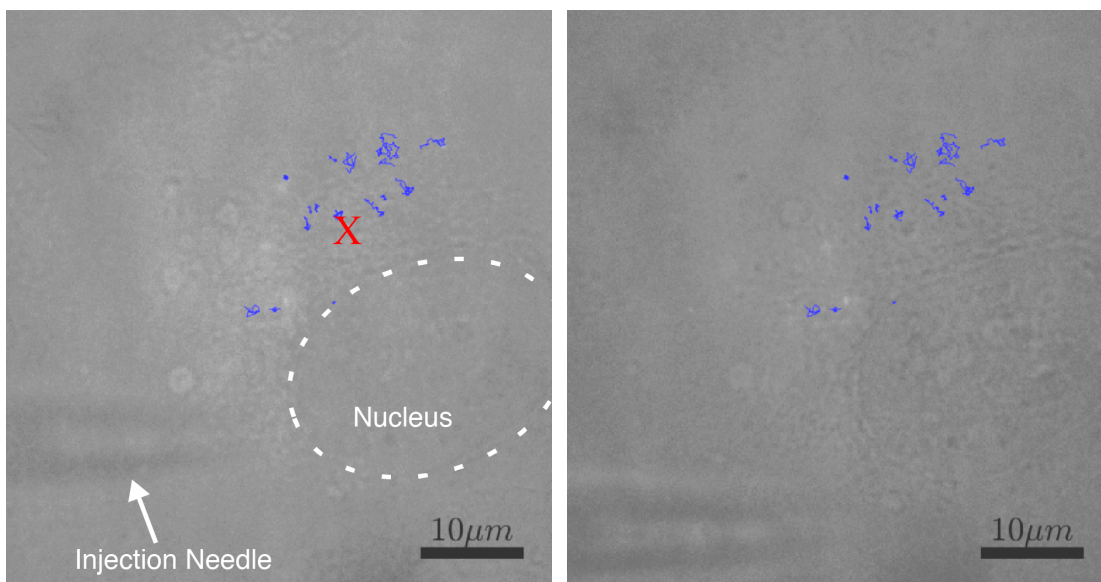


**Figure S11.** Still OM images with particle tracks overlaid for a fibrosarcoma cell before injection (left) and after a time lapse of 2 min post injection (right). Images are extracted from representative movie before cropping the length and compression. Injection location is denoted with a red X.

## References

- (1) Grady, M. E.; Composto, R. J.; Eckmann, D. M., Cell elasticity with altered cytoskeletal architectures across multiple cell types. *J. Mech. Behav. Biomed. Mater.* **2016**, 61, 197-207.
- (2) Lee, C. H.; Crosby, A. J.; Emrick, T.; Hayward, R. C., Characterization of heterogeneous polyacrylamide hydrogels by tracking of single quantum dots. *Macromolecules* **2014**, 47, 741-749.